Imagined 3D Hand Movement Trajectory Decoding from Sensorimotor EEG Rhythms

Attila Korik[1], Ronen Sosnik[2], Nazmul Siddique[1], Damien Coyle[1]
[1] Intelligent Systems Research Centre (ISRC), Ulster University, Derry, UK
[2] Hybrid BCI Lab, Holon Institute of Technology (HIT), Holon, Israel
Email: korik-a@email.ulster.ac.uk

***Abstract* — Reconstruction of the three-dimensional (3D) trajectory of an imagined limb movement using electro-encephalography (EEG) poses many challenges. However, if achieved, more advanced non-invasive brain-computer interfaces (BCIs) for the physically impaired could be realized. The most common motion trajectory prediction (MTP) BCI employs a time-series of band-pass filtered EEG potentials for reconstructing the 3D trajectory of limb movement using multiple linear regression (mLR). Most MTP BCI studies report the best accuracy using low delta (0.5-2Hz) band-pass filtered EEG potentials. In a recent study, we showed spatiotemporal power distribution of theta (4-8Hz), mu (8-12Hz), and beta (12-28Hz) EEG frequency bands contain richer information associated with movement trajectory. This finding is in line with the results in the extensive literature on traditional sensorimotor rhythm (SMR) based multiclass (MC) BCI studies, which report the best accuracy of limb movement classification using power values of mu and beta frequency bands. Here, we show the reconstruction of actual and imagined 3D limb movement trajectory with an MTP BCI using a time-series of bandpower values (BTS model). Furthermore, we show the proposed BTS model outperforms the standard potential time-series model (PTS model). The BTS model yielded best results in the mu and beta bands (R~0.5 for actual and R~0.2 for imagined movement reconstruction) and not in the low delta band, as previously reported for MTP studies using the PTS model. Our results show for the first time how mu and beta activity can be used for decoding imagined 3D hand movement from EEG.**

Keywords — 3D motion trajectory prediction, brain-computer interface (BCI), imagined hand movement, electroencephalography (EEG), motor imagery (MI), sensorimotor rhythms (SMR)

I. Introduction

To date, two different approaches have been used in non-invasive motor imagery (MI) brain-computer interfaces (BCIs). Multiclass (MC) sensorimotor rhythm (SMR) BCIs enable multi-dimensional control in the real or virtual spaces using a classifier trained to distinguish between the imagined movement of different limbs, commonly the left hand, right hand, foot, and tongue [1], or more advanced applications using a self-regulatory scheme in which the user learns to modulate the SMR to gain control over different dimensions independently [2], [3]. In contrast to MC SMR BCIs, common motion trajectory prediction (MTP) BCIs aim to reconstruct the limb movement trajectory itself, i.e., estimate the track of the limb coordinates or velocity vectors during an executed or imagined movement [4]. Commonly, MTP BCI involves decoding a single upper limb movement towards multiple targets in 3D spaces [5], [6], [7], whilst finger movements have also been decoded using a non-invasive MTP technique [8]. The traditional MC SMR BCIs normally involve discrete classification of movements into different classes (e.g., left arm movement vs. right arm movement imagination) [9]. In contrast, MTP BCIs reconstruct the 3D trajectory from a time-series of band-pass filtered EEG potentials using multiple linear regression (mLR) [5], [10]. SMR BCIs report the best accuracy when power values of mu (8-12Hz) and beta (12-30Hz) bands are used for classifying the movement [3], [11], [12]. In contrast, MTP BCIs usually report the best results when a low delta (0.5-2Hz) band-pass filter is applied to the EEG before preparing the input time-series for an mLR-based kinematic data estimation module [5], [7], [8]. As the optimal frequency bands most commonly reported differ for classifying and decoding hand movement using MC SMR BCIs and MTP BCIs, (mu and/or beta vs delta band), respectively, this study aimed to shed light on this contrasting result. In our recent study [13], we showed for the first time that replacing the time-series of bandpass filtered EEG potentials (PTS model) with a time-series of power values (BTS model) from the theta (4-8Hz), mu (8-12Hz), and beta (12-28Hz) bands yields higher MTP accuracy during executed 3D hand movement. Here we report the results of a study that compares the bandpower time-series (BTS) based MTP model with the time-series of bandpass filtered EEG potentials (PTS model) for predicting both executed and imagined movement trajectories. The results show that imagined 3D movements can be decoded from EEG and the results strengthen the case for using bandpower in mLR based MTP BCIs.

This research was supported by Vice-Chancellor's Research Scholarship (VCRS), Intelligent Systems Research Centre (ISRC), Ulster University. Data acquisition was supported by the Israel Science Foundation (grant No. 76/12).

II. Methods

A. Subjects and Paradigm

Four healthy subjects (males, aged 25-46 years) participated in the study. Data was acquired at the Hybrid BCI lab at Holon Institute of Technology (HIT), Israel. The study had full ethical approval from the Wolfson Medical Center Research Ethics Committee. All subjects were right-handed, without any medical or psychological illness and/or medication and had normal or corrected to normal vision. The subjects were informed about the experimental task to be undertaken prior to the experiment. Subjects sat on a chair, 1.5m in front of a 3D Microsoft Kinect camera, looking forward and were requested to maintain a constant head position, refrain from teeth grinding and to minimize unrequired movement during the experiment. They were also asked to minimize eye blinks

during the movement cycles (described below) and to rest during the inter-task resting periods.

The experiment comprised eight runs: four executed movements runs and four imagined hand movements runs. Each executed movement run was followed by an imagined movement run. The runs were separated by one minute inter-run resting (IRR) period. During IRR, the subjects were asked to relax and not to move or talk. The runs comprised repeated (executed or imagined) movements between a home position and one of the four target positions (Fig. 1A).

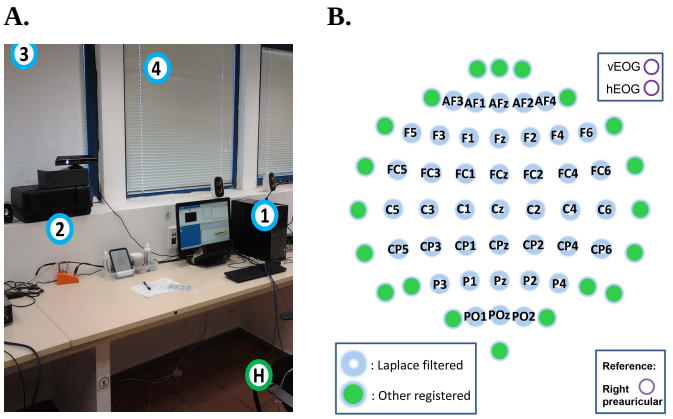

Fig. 1. **A:** Illustration of the experimental setup. The green circle with H and blue circles with numbers indicate the home position and four target positions, respectively. **B**: Illustration of EEG montage and the channel locations that were used as center points for the Laplace filtering.

Targets 1 and 2 lay in the shoulder plane forming 60° and 0°, respectively, between the torso and the shoulder. Targets 3 and 4 lay 30° above the shoulder plane, forming 0° and 60°, respectively, between the torso and the shoulder. The format of the executed and imagined runs is presented in Fig. 2.

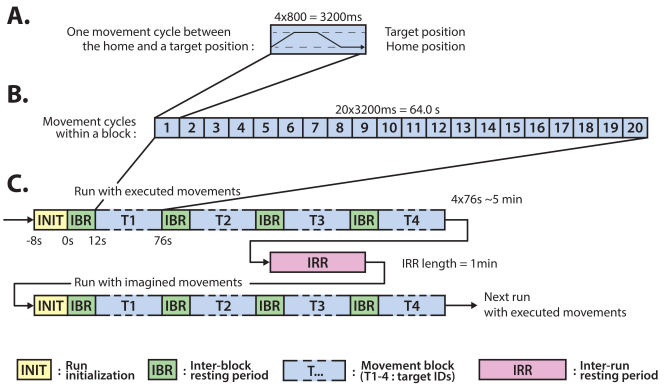

Fig. 2. The timing of the experimental paradigm. **A**: timing of an executed or imagined movement cycle between the home position (H) and one of the four targets (T1-4); **B**: structure of one block comprising 20 movement cycles between the home position and one of the four targets; **C**: structure of a run for imagined and executed movements, wherein a run comprises four blocks corresponding to each of the four targets (T1-4).

Each run comprised four blocks, each comprising twenty executed or imagined hand movements between the home position and one of the four targets. Eight seconds before run initiation, the subject was asked to get ready for the task. The movement between the home position and a target was synchronized with an 800ms auditory cue (6 kHz tone), which was followed by an 800ms pause epoch. The backward movement from the target to the home position was synchronized with an 800ms auditory cue (4 kHz tone), which was followed by an 800ms resting epoch at the home position. Thus, a movement cycle lasted for 3200ms (Fig. 2A), a movement block lasted for 48 seconds (Fig. 2B), and a run lasted five minutes, comprising four blocks, each followed by an inter-block resting (IBR) period lasting twelve seconds (Fig. 2C). For each IBR, a recorded voice message was played four seconds before the next block initiation, informing the subject about the following target. The runs were separated by an inter-run resting (IRR) period lasting one minute.

For imagined movement runs the experiment timing was identical but the user was asked to kinaesthetically imagine the movement of the hand towards each target.

B. Data Acquisition

EEG and kinematic data were acquired from the subject simultaneously. EEG signals were registered in 61 channels and two electrooculogram (EOG) channels at 1200 Hz using an 80 active channels g.HIamp80 EEG system (g.tec medical engineering GmbH, Schiedlberg, Austria). The EEG reference electrode was positioned on the right ear lobe. The EEG was amplified (gain: 20000), filtered (Butterworth 0.5-100Hz, 8^{th} order), and sampled (A/D resolution: 24 Bits, sampling rate: 1200 samples/s). The ground electrode was positioned on the forehead above the nose. Impedance for all active electrodes was below 50KΩ. The 3D Microsoft Kinect camera system was developed for the Xbox 360 to record 3D limb movements. We decided to use this device for registering kinematic data as it provides 3D coordinates of limbs' joints with sufficient accuracy. Kinematic data were recorded from the right dominant hand, elbow, and shoulder at 30 frames per second (FPS). The kinematic data acquisition does not require placing markers on the joints of the arm because the Kinect camera system can identify the limb joints without markers.

C. Preprocessing

EEG was re-referenced using a small Laplace filter to reduce common mode artifacts. The small Laplace filter was processed on the 41 center electrode locations presented in Fig. 1B. The baseline of the re-referenced EEG signals was shifted to zero at each electrode. Preprocessed EEG data intervals with a high-level transient noise ($>|\pm 300\mu V|$) were removed from further analysis and a 0.5-40Hz, an 8^{th} order Butterworth filter was applied for filtering out non-relevant frequency bands before independent component analysis (ICA) was applied. The ICA was performed on the 41 preprocessed channels for removal of electrooculogram (EOG) and electromyogram (EMG) artifacts, and for noise reduction. As outlined above, two models for time-series analysis were applied: the potential time-series (PTS) model and the bandpower time-series (BTS) model. After the ICA, for the PTS model, the data were parallel filtered by six non-overlapped, 8^{th} order band-pass filters in the following six frequency bands: lower delta (0.5-2Hz), theta (4-8Hz), mu (8-12Hz), lower beta (12-18Hz), upper beta (18-28Hz), and gamma (28-40Hz). In the case of the BTS model, the time varying bandpower was calculated for each of

the six non-overlapped EEG bands based on the ICA filtered EEG signals. The bandpower was calculated in 500ms width sliding time windows, with a 33.3ms time lag between two adjacent windows. This time lag was chosen to match the kinematic sampling rate (30FPS). The bandpower within a time window was calculated by averaging the absolute values of the band-pass filtered EEG potentials within the window as described by

$$B_{fn}[t] = \frac{\sum_{m=1}^{M} |S(m)_{fn}[t]|}{M} \quad (1)$$

where $B_{fn}[t]$ is the bandpower value calculated from EEG channel *n*, using band-pass filter *f*, within a 500ms width time window *t*. *M* is the number of samples within a time window and *S(m)* is the m[th] band-pass filtered sample within the time window. Thus, the BTS model was trained separately with the time-series of bandpower values that were calculated from the ICA filtered EEG in each of the following six frequency bands: 0.5-4Hz, 4-8Hz, 8-12Hz, 12-18Hz, 18-28Hz, and 28-40Hz. The performance for each band was compared for both the PTS and BTS models (see section II.E for training, cross-validation, and testing).

The registered kinematic data were charged with high-frequency noise (>10Hz), which did not originate from real movement. This noise was reduced before further processing. As low-pass filtering would cause a significant distortion in the kinematic data during the movement periods, a moving average smoothing filter with a five sample window was applied separately for each kinematic coordinate. Data intervals that were charged with a high-level transient noise (verified by manual inspection) were marked and removed from further processing along with their corresponding EEG data.

Based on the registered kinematic data, the onset and the offset trigger points of each block were registered manually in each run to trigger the data.

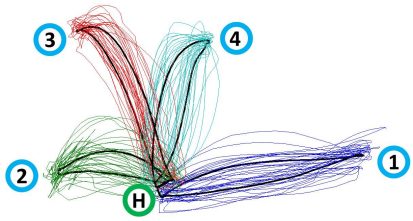

Fig. 3. Illustration of registered (color) and averaged (black) 3D hand movement trajectories between the home position (green circle with H) and four target positions (blue cicles with numbers) using kinematic data of subject 1, run 1.

As there is no registered kinematic data in the imagined movement runs, estimated kinematic data were calculated by averaging the kinematic data in the executed movement run prior to the corresponding imagined movement run. The averaged trials were calculated separately for each block, which involved data for different targets (Fig. 3). The onsets of the trials were identified by the stored triggers based on the onset of the auditory cues.

D. Kinematic Data Reconstruction

The core module in an MTP BCI is the kinematic data estimator block, which reconstructs the kinematic trajectory based on the input EEG time-series. In the training stage, the key parameters of the estimation block are optimized. Fig. 4 illustrates the configuration for training the estimation block in order to attain maximal correlation between the registered and reconstructed trajectories.

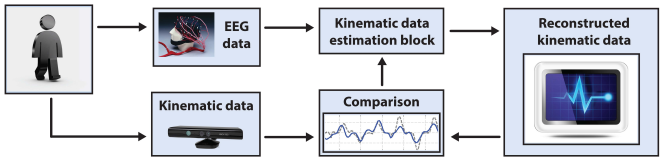

Fig. 4. Structural elements for training an MTP BCI.

The mLR-based PTS model was presented by Bradberry et al. [5] as described by

$$x_i[t] = a_{if} + \sum_{n=1}^{N} \sum_{k=0}^{L} b_{ifnk} S_{fn}[t-k] + \varepsilon[t] \quad (2)$$

where a_{if} and b_{ifnk} are regression parameters that learn the relationship between $S_{fn}[t-k]$ input and $x_i[t]$ output data. $x_i[t]$ contains the three orthogonal velocity components, $S_{fn}[t-k]$ is standardized temporal difference of EEG potentials on which band-pass filter *f* is applied at EEG sensor *n* at time lag *k* according to (2). The *i* index denotes spatial dimensions in the 3D orthogonal coordinate system, *N* is the number of EEG sensors, *L* is the number of time lags, and ε[t] is the residual error. The embedding dimension (or model order) is the number of time lags plus one (*L+1)*, i.e., the number of time lagged samples that are selected from each channel for estimating kinematic data at time point *t*. The standardized difference for the PTS model is

$$S_{fn}[t] = \frac{P_{fn}[t] - \mu_{P_{fn}}}{\sigma_{P_{fn}}} \quad (3)$$

where $P_{fn}[t]$ is the value of the input time-series at time *t* (i.e., a potential value for the PTS model), $\mu_{P_{fn}}$ is the mean value, and $\sigma_{P_{fn}}$ is the standard deviation of P_{fn}.

The BTS model presented here uses the same equation for mLR as described for the PTS model in (2) but the standardized temporal difference $S_{fn}[t-k]$ is calculated from bandpower values of the specified EEG band, rather than band-pass filtered EEG potentials. As bandpower values are limited to the positive value range, the standardized difference was calculated differently for the PTS model (3) for which the input was roughly symmetric. The standardized difference for the BTS model is

$$S_{fn}[t] = \frac{B_{fn}[t]}{\sigma_{B_{fn}}} \quad (4)$$

where $B_{fn}[t]$ is the value of the input time-series at time t (i.e., a bandpower value for the BTS model) and $\sigma_{B_{fn}}$ is the standard deviation of B_{fn}.

In the case of the PTS and BTS models, the input-output structure of the kinematic data estimation module is similar. The only difference is the optimal number of time lags (i.e., embedding dimension minus one) that is selected during parameter optimization as described in the following section.

E. Parameter Optimization

An inner-outer cross-validation (CV) technique was employed for parameter optimization. This method allows optimizing the MTP architecture by testing and selecting a range of parameters using the inner fold CV and calculating the final results based on the outer test folds using the optimal architecture selected in the inner fold CV. Further details of the inner-outer CV technique can be found in [13]. The MTP accuracy is assessed by estimating the correlation between the measured and the reconstructed kinematic trials. The final results were calculated by averaging MTP accuracy across the outer folds for each subject, separately. We applied a six-fold CV on the inner folds and seven-fold CV in the outer folds.

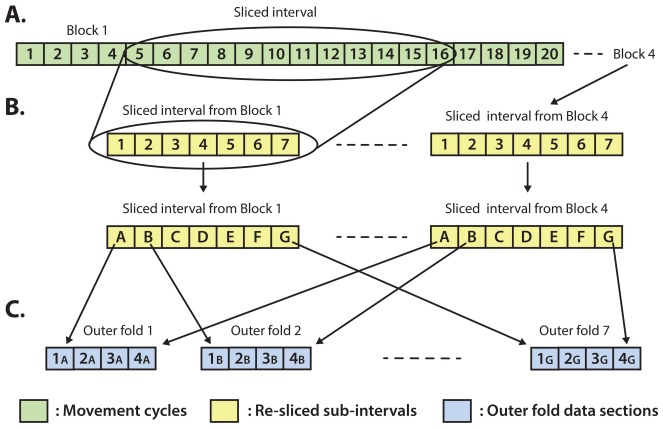

Fig. 5. The structure of the outer folds based on the recorded data structure. **A**: block with 20 repeated movement cycles, **B**: separated sub-intervals of the selected movement cycles (1-7) and the same sub-intervals in randomized order (A-G), **C**: homogeneous distribution of sub-intervals in outer folds.

The analyzed dataset involved four runs for each task (i.e., executed or imagined movement), each run comprised four separate blocks for each of the four targets, and each block comprised twenty movement cycles between the home position and one of the targets as illustrated in Fig. 2. A forty seconds length interval, comprising approximately twelve movement cycles, centered at the middle of each block was selected for further processing as shown in Fig. 5A. Each forty seconds interval slice was divided into seven non-overlapping sub-intervals and then the order of the sub-intervals within each slice was randomized separately, as presented in Fig. 5B. From this data structure, the sub-intervals were re-distributed into seven outer folds as illustrated in Fig. 5C (i.e., the data for each outer fold were drawn from four unique movement intervals, with a similar length for each of the four targets). This kind of data separation guaranteed the homogenous distribution of movement dependent data intervals for each outer fold.

As the global parameter space is too large for one-step optimization, i.e., there are multiple parameters that can affect performance, it is a challenge to optimize globally. A three-step approach was taken for optimization, as described in [13]. In the first optimization phase, the EEG montage was fixed, whilst time lag and embedding dimension were optimized. The second optimization phase used the parameters optimized in the first optimization phase, whilst the importance of channels was identified by evaluating all single channels independently, ranking channels by their importance and selecting a subset. The third phase involved re-optimization of time lag and embedding dimension with the chosen subset of channels from the second phase of optimization. The optimal configuration was identified by a heuristic global search method. The optimization was conducted separately for all combinations of the following options for the two models (PTS and BTS): four subjects, four runs, executed and imagined movements, three spatial dimensions, six frequency bands, and 7x6 inner-outer fold combinations. The investigated parameter space is presented in Table1.

TABLE I. RANGE OF THE PARAMETER SPACE USED IN THE INNER LEVEL TO IDENTIFY THE OPTIMAL SETUP FOR OUTER TESTS.

Parameter	**Investigated parameter space**	
	PTS model	***BTS model***
Time lag	33ms … 300ms	33ms … 600ms
Embedding dimension	1 … 12 samples	1 … 12 samples
Input frequency band	0.5-2Hz, 4-8Hz, 8-12Hz, 12-18Hz, 18-28Hz, 28-40Hz	0.5-4Hz, 4-8Hz, 8-12Hz, 12-18Hz, 18-28Hz, 28-40Hz

The optimal time lag, embedding dimension, and most prominent frequency bands were selected in the inner-fold CV. Accuracy metrics (i.e., correlation value) of the hand velocity trial reconstruction was calculated separately for the PTS and BTS models in the selected frequency bands for the seven outer test folds and three orthogonal vector components in x, y, and z directions. The mean value of the accuracies calculated across the seven outer test folds was averaged and compared for the executed and imagined movement using the PTS and BTS models for each of the three directions, respectively. Statistical differences were analyzed using the student's *t*-test.

III. RESULTS

The optimal time lag for the PTS model was selected to be approximately 100…150ms. For the BTS model, it was around 300ms. The optimal embedding dimensions (i.e., time lag number +1) for both models was 11. The topological distribution of the cortical areas, which resulted in the highest accuracy in the inner fold tests using single input channel setups, varied significantly but the test results for executed and imagined movement using the same configuration showed similar topological results. The most prominent cortical area for the PTS model was identified typically in the sensorimotor cortex while it shifted between the sensorimotor cortex and the posterior cortical areas for the BTS model.

Figures 6-9 present a comparison of the accuracy for executed and imagined hand movement trajectory

reconstruction based on the six investigated input frequency bands across each of the four subjects (the accuracies from four runs, seven outer folds, and three spatial dimensions were averaged separately for each subject and frequency band).

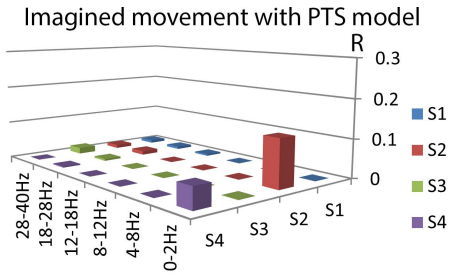

Fig. 6. Accuracy of MTP for imagined movements using the PTS model in the six analyzed input frequency bands for the four investigated subjects (S).

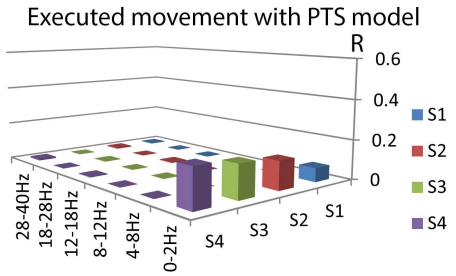

Fig. 7. Accuracy of MTP for executed movements using the PTS model in the six analyzed input frequency bands for the four investigated subjects (S).

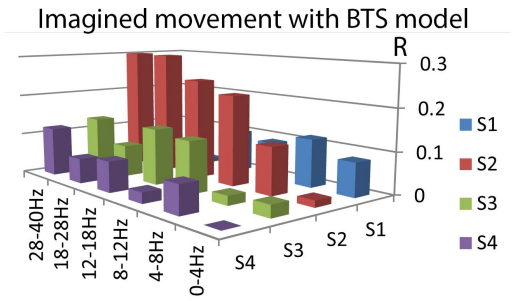

Fig. 8. Accuracy of MTP for imagined movements using the BTS model in the six analyzed input frequency bands for the four investigated subjects (S).

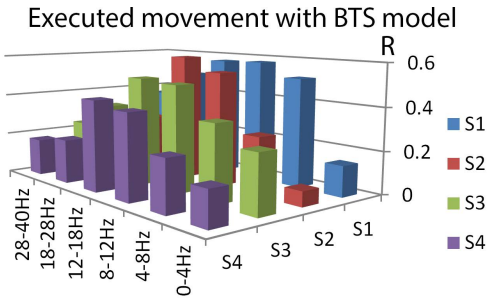

Fig. 9. Accuracy of MTP for executed movements using the BTS model in the six analyzed input frequency bands for the four investigated subjects (S).

Finally, Fig. 10 presents an example of the average actual and reconstructed kinematic velocity profile for imagined hand movements using the BTS model.

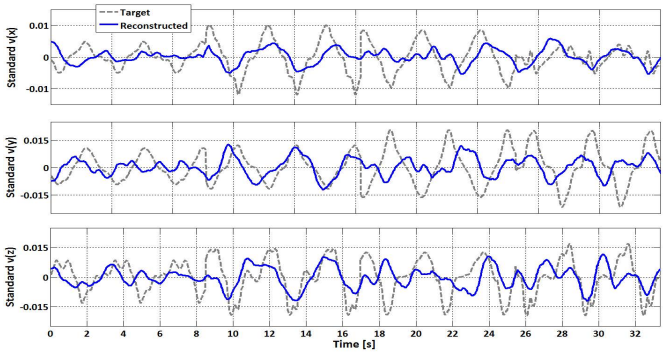

Fig. 10. Illustration of the average actual and reconstructed hand velocity profile for the imagined movement task (based on Subject 2, Run 4, 12-18Hz, outer fold 4 test result).

IV. Discussion

MTP BCIs commonly use the time-series of band-pass filtered EEG potentials for trajectory reconstruction of an executed movement. Here we show that the trajectory of an imagined hand movement can also be decoded from the EEG signal. In additional, we compared the accuracy of the standard PTS MTP model [5] and the recently introduced BTS MTP model [13], [14] on both, executed and imagined, movement.

The results obtained are in line with our expectations. The BTS model provided significantly higher (p<0.05) accuracy compared to the PTS model (Fig. 6-9). The accuracy of the PTS model was maximal in the low delta band (0-2Hz) for both movement types (imagined and executed) (Fig. 6-7) and was very low for other bands. In line with our recent studies [13], [14], the BTS model in the mu (8-12Hz) and beta (12-28Hz) bands provided the highest accuracy (R~0.5) (Fig. 9). The 8-30Hz activity is dominantly used in traditional multiclass (MC) SMR BCIs [1], [2], [3] whilst most of the MTP BCI studies have focused on low delta band.

The accuracy of the imagined movement reconstruction (R~0.2) (Fig. 8) was significantly lower than that of for the executed movement (R~0.5). The BTS model provided higher accuracy compared to the PTS results for both executed and imagined movements. In the case of the imagined movement tasks the BTS MTP achieved the highest accuracy in the mu (8-12Hz), beta (12-28Hz), and low-gamma (28-30Hz) bands. Thus, the BTS model provided the highest accuracy for the imagined and executed movements in slightly different bands, but the mu and beta bands in the both cases were dominant. Topological distribution of the single EEG channel tests showed similar results in the case of the executed and imagined movement tasks. In the case of the PTS model the sensorimotor cortex provided the highest accuracy, as expected. In the case of the BTS model, the most prominent cortical areas were identified between the sensorimotor and the posterior cortical areas.

Our result showing that, 8-28Hz band is optimal for reconstructing the trajectory of an imagined or executed movement reconciles the traditional SMR BCI models with the MTP BCIs, as both approaches provide the highest accuracy in similar bands. In [13] we provided an explanation of why the kinematic trial reconstruction by the PTS MTP model is only successful when the input time-series is filtered in the delta

band. We showed that the input time-series should cover similar time interval that is determined by the rhythms of the movement and the time lag should be scaled to the time-varying movement relevant changes in the cerebral-activity. In the case of the optimal time lag (~100...300ms), the band-pass filtered EEG signals are represented well by the input time-series if, and only if, the band-pass filter is applied to the 0.5-2Hz frequency range. If the band-pass filter is applied to a higher (>4Hz) frequency range, the input PTS is composed of quasi-random potential values because the width of the time lag is longer than the time period of the band-pass filtered EEG signals and aliasing of the higher frequency filtered signals occurs. In contrast, the BTS model has access to the spatiotemporal EEG power pattern in any specific frequency band, as the input BTS is composed of time-varying bandpower values (at the selected EEG sensor locations). As the BTS input using the optimal time lags can follow the alternation of the bandpower values, the spatio-temporal power pattern of the EEG is represented properly by the BTS in any EEG frequency band (more details in [13]).

In order to confirm the reconstructed trajectories are valid, a target shuffling test was performed, wherein different types of movement cycles were shuffled in the kinematic test dataset. Trajectories were reconstructed in the same way for both, un-shuffled and shuffled datasets from each of the outer folds. The correlation in the case of the shuffled kinematic data for all folds was close to zero (R~0) as expected for shuffled targets. The difference of un-shuffled (R~0.5) and shuffled (R~0) test results is significant and provide clear evidence that the methods applied and results attained here are not caused by random fluctuations in the data nor are the evaluation methods applied suboptimal.

Although the accuracy of the MTP is significantly improved by replacing the PTS model ($R_{executed}$ ~ 0.2) with the BTS model ($R_{executed}$ ~ 0.5), the obtained accuracy rates are relatively low compared to a number of studies reporting accuracy rates of R~0.3-0.7 for executed hand movement reconstruction using the standard PTS method ([5], [6], [15]). This difference may originate from a relatively high noise level that was identified in the EEG records. We are working to improve the quality of our EEG records in order to increase the signal-to-noise ratio (SNR). An over sensitive ICA component removal could also have an impact where, in some cases, executed movement could have some influence on the signals in low-frequency bands, i.e., actual physical movement could cause an effect on the electrodes. In our case, ICA is applied to remove any such distortions whereas the other cited studies do not report results with ICA. Additionally, to the best of the authors knowledge, there has been no evidence yet that low-frequency delta band provides valuable information for imagined 3D movement reconstruction nor in traditional MC SMR BCIs. We have shown that only a limited amount of information is available in the delta band for two subjects (R<0.1), therefore, even though executed movements can be decoded using low-frequency band information, low-frequency decoding may not be feasible for BCIs, which traditionally are targeted at physically impaired users who require movement–free communication and control.

V. Conclusion

This study aimed to build on our earlier work [13], [14] showing EEG mu and beta bands encode information for 3D hand movement trajectory reconstruction. Here we show for the first time that imagined 3D hand reaching movements can be decoded from mu, beta and gamma activity using a bandpower time-series (BTS) model and multiple linear regression.

This work is an encouraging step towards the development of non-invasive BCI based artificial or robotic limb movement control.

References

[1] G. Pfurtscheller et al., "Mu rhythm (de)synchronization and EEG single-trial classification of different motor imagery tasks.," *Neuroimage*, vol. 31, no. 1, pp. 153–9, May 2006.

[2] A. S. Royer et al., "EEG control of a virtual helicopter in 3-dimensional space using intelligent control strategies.," *IEEE Trans. Neural Syst. Rehabil. Eng.*, vol. 18, no. 6, pp. 581–9, Dec. 2010.

[3] J. R. Wolpaw and D. J. McFarland, "Control of a two-dimensional movement signal by a noninvasive brain-computer interface in humans.," *Proc.Natl.Acad.Sci.*, vol.101, no.51, pp.17849–54, Dec. 2004.

[4] A. Korik et al., "Brief review of non-invasive motion trajectory prediction based brain-computer interfaces," in *8th IEEE EMBS UK & RI PG Biomed. Eng. & Medical Physics, Warwick*, p. 2, pp. 23-24, 2014.

[5] T. J. Bradberry et al., "Reconstructing three-dimensional hand movements from noninvasive electroencephalographic signals," *J. Neurosci.*, vol. 30, no. 9, pp. 3432–7, Mar. 2010.

[6] K. Choi, "Reconstructing for joint angles on the shoulder and elbow from non-invasive electroencephalographic signals through electromyography.," *Front. Neurosci.*, vol. 7, no. Oct, p. 190, Jan. 2013.

[7] H. G. Yeom et al., "Estimation of the velocity and trajectory of three-dimensional reaching movements from non-invasive magnetoencephalography signals.," *J. Neural Eng.*, vol. 10, no. 2, p. 026006, Feb. 2013.

[8] A. Y. Paek et al, "Decoding repetitive finger movements with brain activity acquired via non-invasive electroencephalography," *Front. Neuroeng.*, vol. 7, no. 3, p, 2014.

[9] D. Coyle et al., "A Time-Frequency Approach to Feature Extraction for a Brain-Computer Interface with a Comparative Analysis of Performance Measures," *EURASIP J. Adv. Signal Process.*, vol. 2005, no. 19, pp. 3141–3151, 2005.

[10] A. P. Georgopoulos et al, "Magnetoencephalographic signals predict movement trajectory in space.," *Exp. Brain Res.*, vol. 167, no. 1, pp. 132–5, Nov. 2005.

[11] D. Coyle et al., "Predictive-Spectral-Spatial Preprocessing for a Multiclass Brain- Computer Interface," pp. 18–23, 2010.

[12] D. J. McFarland et al., "Mu and beta rhythm topographies during motor imagery and actual movements," *Brain Topogr.*, vol. 12, no. 3, pp. 177–86, Jan. 2000.

[13] A. Korik et al., "3D Hand Motion Trajectory Prediction from EEG Mu and Beta bandpower," in *PBR: Brain-Computer Interfaces: Lab Experiments to Real-World Applications*, D. Coyle, Ed. Elsevier Inc., 2016. [in press]

[14] A. Korik et al., "3D Hand Movement Velocity Reconstruction using Power Spectral Density of EEG Signals and Neural Network," in *35th Annual International Conference of the IEEE Engineering in Medicine and Biology Society, Milan*, pp. 8103–8106, 2015.

[15] J. Liu et al., "Hand movement decoding by phase-locking low frequency EEG signals.," in *Conf. Proc. IEEE Eng. Med.Biol. Soc.*, 2011, vol, pp. 6335–8, 2011.

[16] P. Ofner and G. R. Müller-Putz, "Decoding of velocities and positions of 3D arm movement from EEG.," *Conf. Proc. IEEE Eng. Med. Biol. Soc.*, vol. 2012, pp. 6406–9, Jan. 2012.